



Palaeoclimate and palaeoseismic events discovered in Diexi barrier lake on the Minjiang River, China

X. Q. Wang¹, Y. R. Li^{2,3}, Y. Yuan¹, Z. Zhou¹, and L. S. Wang¹

¹State Key Laboratory of Geohazard Prevention and Geoenvironment Protection (Chengdu University of Technology), Chengdu 610059, China

²Taiyuan University of Technology, Taiyuan 030024, China

³AGECON Ltd., Hong Kong, China

Correspondence to: Y. R. Li (li.dennis@hotmail.com)

Received: 16 February 2014 – Revised: – Accepted: 10 March 2014 – Published: 14 August 2014

Abstract. Studies on the formation of the ancient Diexi barrier lake on the Mingjiang River, southwestern China, have long been carried out. However, investigations into the correlation between the palaeoclimate and palaeoenvironment and the palaeoseismic events in this area are rarely found in literature. The present study took sediments from the ancient Diexi barrier lake to investigate the palaeoclimate, palaeoenvironment and palaeoseismic events. A drilling at the centre of the barrier lake was conducted and the core of about 260 m long was examined. The palaeoclimate and palaeoenvironment indicators (sporopollen, carbon and oxygen isotopes, organic matter, calcium carbonate, granularity) from the sediments have been tested and analysed, and indicate that there were 10 climatic and environmental periods between 30 000 and 15 000 a BP (before present). The discovered disturbance segments in the core indicate there were at least 10 seismic events during that period. The consistency between climate change and seismic events indicates that a strong seismicity is normally accompanied by a climatic variation. This may be a useful supplement for climate and geohazard predictions in the future.

1 Introduction

The foreign matter caused by rockfall, landslide, debris flow and lava flow often clog a river by forming a barrier on it. Earthquakes are normally one of the main causes of rockfall, landslide and mudflow (Huang et al., 2008). The ancient barrier lake refers to the remains formed by such events a long time ago. Previous studies about the barrier lake mainly

focused on the formation mechanism and stability of the barrier and the environment change with the life of the barrier. Weidinger (1998) investigated the stability of the landslide barriers located in the Himalayas. Trauth and Strecker (1999) dated the formation time of the landslide barrier lake located in northwestern Argentina. Wassmer et al. (2004) investigated the landslide barrier lake located in the Rhine Valley of Switzerland and the research was mainly focused on the failure mechanism of the barrier. Krivonogov (2005) studied the ice-dammed lake located in northern Mongolia and focused on the formation time of the barrier and the environment during the time when the lake existed. Moreiras (2006) investigated the approximate formation time of the landslide barrier lake located on the Cordón del Plata River of in the central Andes and he considered the clogging event related to seismicity, together with climatic conditions, rock formations and geological structures. Yang et al. (2005) investigated the evolution of the ancient barrier lake in the Diexi area by analysing the lithology and sediment system. An et al. (2008) considered that the lacustrine deposit of the ancient barrier lake along the Minjiang Fault reflects the tectonic activities of the fault. Zhang et al. (2009) investigated the climatic variation associated with the Diexi's ancient dammed lake by AMS (accelerator mass spectrometry)-¹⁴C dating and granulometry. They divided the evolution of the palaeoclimate in the research area into three stages: stage I (40.5–33.4 ka BP – before present) being cold and dry climate, stage II (33.4–31.7 ka BP) being warm and humid, and stage III (31.7–31.1 ka BP) being relatively warm and humid. Wang et al. (2000, 2005, 2007, 2009) studied the geological environment and climatic evolution by dating the deposits in

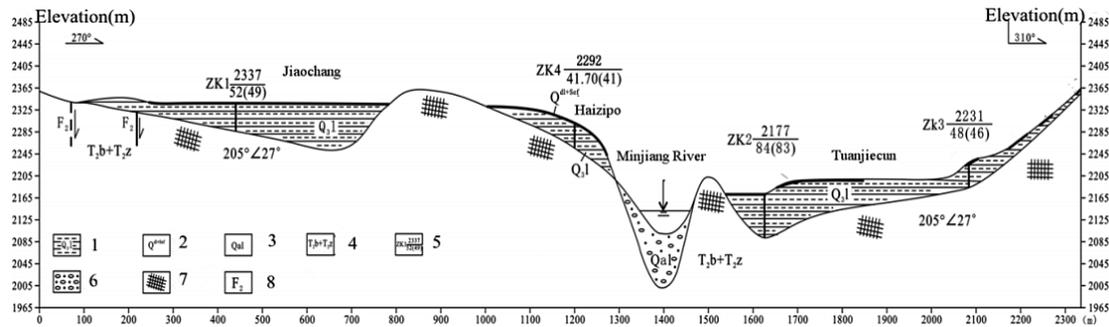


Figure 3. Typical cross section of the Diexi barrier lake (Section III–III' in Fig. 2.)



Figure 4. Structure of lacustrine sediment in the Diexi barrier lake.

systems are widely spread in the Minjiang River regions. The Jiaochang Formation with a mountain-shaped arcuate structure is of several hundred metres wide (Fig. 1).

The Diexi ancient barrier lake is located in the deep V-shaped gorge region of the Minjiang River (Fig. 2), where mountains are high, the gorge is deep and the river current is fast with an average water surface gradient of about 10.3%. The thickness of the sediment in the middle of the barrier lake near the Tuanjie and Jiaochang villages is about 200 m. The age of the sediments at the bottom is about 30 000 a and of those at the top about 15 000 a.

The barrier dam was formed by a series of landslides that originated from the bank slopes. As shown in Fig. 3, the top elevation of the lake sediments is about 2340 m a.s.l. The thickness of the sediments near Tuanjie and Jiaochang villages is greater than 200 m. In this area, the sediments are silty clay. At the tail of the barrier lake in Taiping Village (Fig. 2) the particle size is greater, showing a fluvial deposit feature. The sediments in the lake centre consist mainly of layered silty sands and clay with clear colour variation (Fig. 4). The thickness of the lamina is 2–5 cm.

3 Methodology

Four drillings (ZK1, ZK2, ZK3 and ZK4) were carried out in the Jiaochang and Tuanjie area, the central part of the ancient Diexi barrier lake. The depth and top elevation of the four drill holes are 52, 84, 48 and 41.7 m, and 2337, 2177, 2231 and 2292 m a.s.l., respectively. The drilling core, in total 216 m long, was well photographed and recorded. In order to obtain the environmental information recorded in the sediment, soil samples were taken at every 4 m from the core and in total 53 samples were collected. Each sample was divided into three parts for spore-pollen and organic-matter testing to extract the climatic information during the process of sediment deposition. In addition, 108 soil samples were taken from the core at every 2 m. Each sample was divided into three parts for testing of carbon and oxygen isotopes, calcium carbonate and particle size distribution, respectively. A dating test was carried out on the core at the soleplate altitude and the top for determining the sediment formation and extinction times.

All tests were carried out according to Chinese standards as listed in the reference list. The sporopollen tests followed SY/T 5915-2000; the stable carbon and oxygen isotope tests were based on SY/T 5915-2000; organic matter tests were according to NY/T85-1988; soil carbonate was based on calcium carbonate tests NY/T86-1988; particle size distribution followed GB/T50123-1999; and dating tests were according to AMS-¹⁴C.

4 Results

4.1 Palaeoclimatic indicators

In total, 12 532 sporopollens of 46 kinds are identified from the tests. The content distribution of sporopollen along the elevation is shown in Fig. 5. The arboreal sporopollen comprises the dominant content of about 59.9–89.1% with an average of 76.2%. Shrubby and herbaceous sporopollen is second with the content of 6.7–36.9% and average of 16.9%. Ferny spores and algal sporopollen rank third with the content of 0.9–17.0% and average of 6.9%. The arboreal

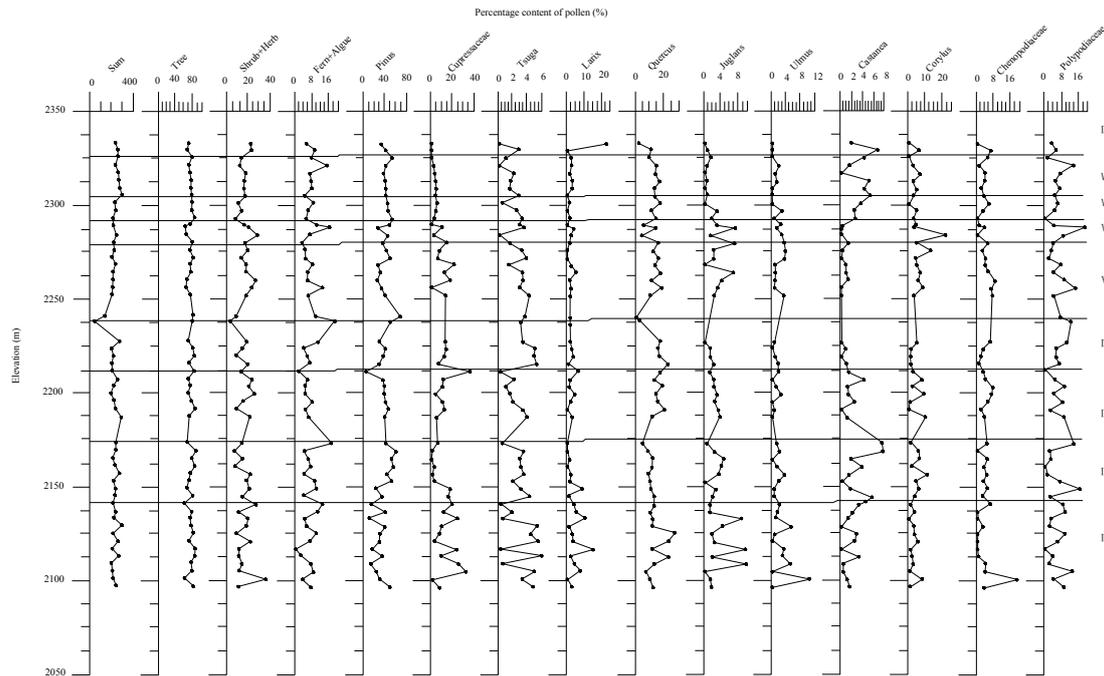


Figure 5. Pollen and spore schema with elevation.

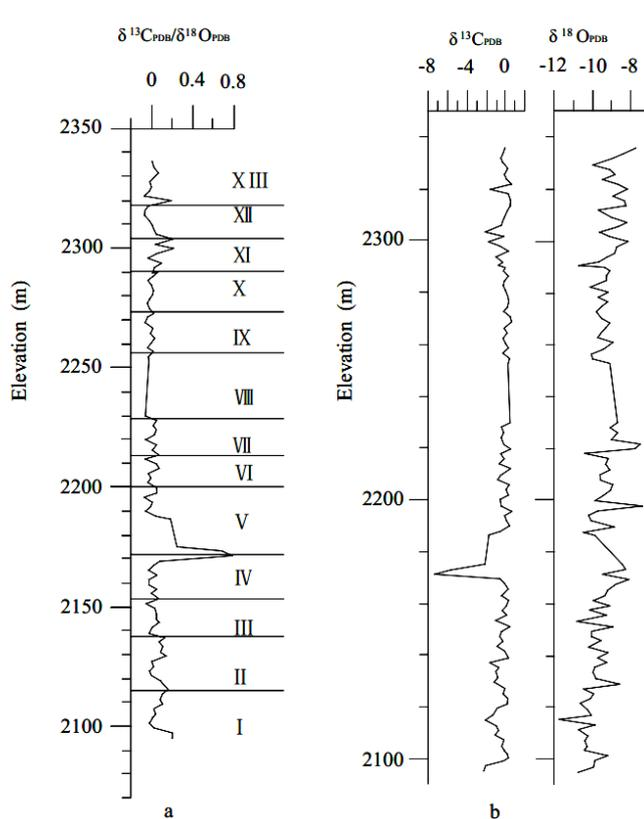


Figure 6. Carbon and oxygen isotopes: (a) ratio of $\delta^{13}\text{C}$ to $\delta^{18}\text{O}$; and (b) values of $\delta^{13}\text{C}$ and $\delta^{18}\text{O}$.

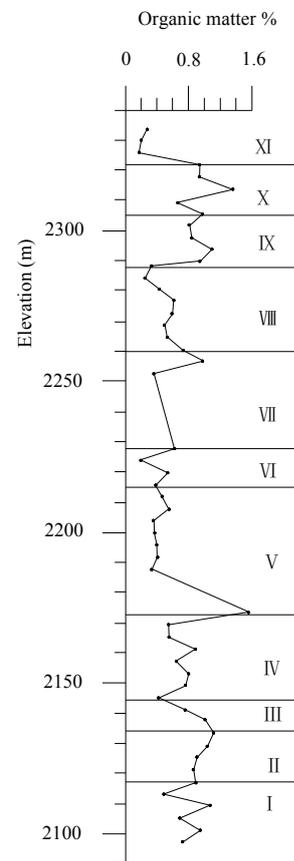


Figure 7. Average content of organic matter.

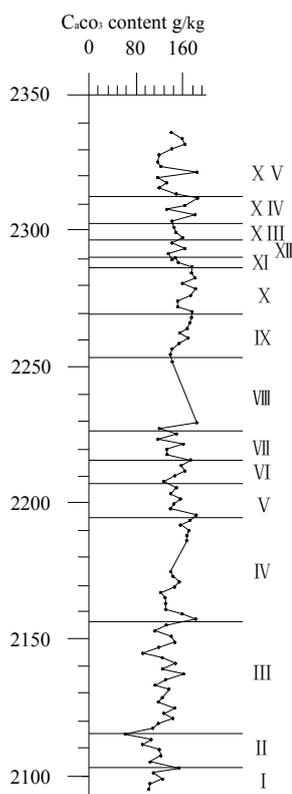


Figure 8. Content of CaCO_3 with elevation.

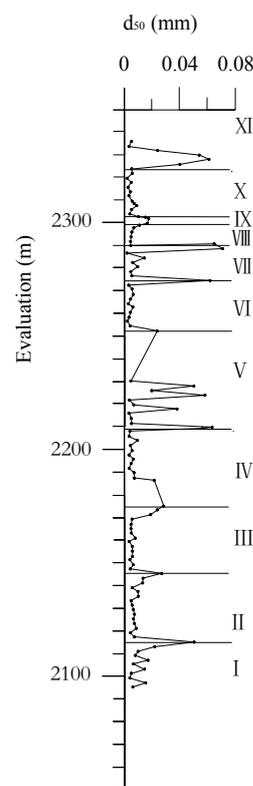


Figure 9. Mean particle size, d_{50} .

pollens mainly include *Pinus*, Cupressaceae and *Quercus* with little *Picea/Abies*, *Tsuga*, *Ulmus*, *Betula*, *Juglans*, *Tilia* and *Carya*. The shrubby and herbaceous pollens include *Corylus*, *Ephedra*, Ericaceae, *Artemisia*, Chenopodiaceae, Gramineae, Liliaceae and Cyperaceae. The ferny spore and algal pollens include Polypodiaceae and Concentricystis.

As shown in Fig. 6, the maximum value of $\delta^{13}\text{C}$ is 0.66 and the minimum is -7.35 , with an average of -0.43 . The maximum value of $\delta^{18}\text{O}$ is -7.44 and the minimum is -11.72 , with an average of -9.42 . The ratio of $\delta^{13}\text{C}$ to $\delta^{18}\text{O}$ ranges from 0.77 to -0.08 , with an average of 0.05. It is noted in Fig. 6 that both $\delta^{13}\text{C}$ and $\delta^{18}\text{O}$ show the similar variation pattern along the elevation.

In the entire elevation profile, the maximum value of the organic matter content is 1.57% and the minimum is 0.17%, with an average of 0.68% (Fig. 7). According to the variation of the content, the whole profile can be divided into 11 segments (segments I–XI). As shown in Fig. 8, the maximum content of the calcium carbonate (CaCO_3) is 187.04 g kg^{-1} and the minimum is 58.66 g kg^{-1} , with an average of 141.49 g kg^{-1} in the entire elevation profile. According to the variation of the content of CaCO_3 , 15 segments can be identified along the elevation profile.

The mean particle size, d_{50} , is presented in Fig. 9 along the elevation. The maximum value of the mean particle size is 0.071 mm and the minimum is 0.002 mm, with an average of

0.013 mm. The distinct variation of d_{50} divides the elevation profile into 11 segments. Through the dating according to the method of AMS- ^{14}C , the year at 2094 m a.s.l. is 30 830 a BP and that at 2306 m is 16 902 a BP.

4.2 Disturbance segments in the drilling core

Through visual examination of the drilling core, 10 segments are identified as they show disturbance structures similar to those shown in Fig. 10. These disturbed segments typically have the following features: (1) wavy and wrapping structure is popular; (2) the laminae vary in thickness; and (3) the disturbed structure is sandwiched by the neighbouring upper and lower horizontal layers.

As shown in Fig. 11a, the wrapping structure is a kind of structure formed by the flow of seismic liquefaction under an unconsolidated condition (Sims, 1975). Fig. 11b presents a flame structure in a single layer, which is confined by horizontal stratification at the top, indicating a younger lacustrine deposit after the disturbance. This kind of disturbance exposed in the drilling core and outcrop is thought to be the product of earthquake vibrations, which liquefy the unconsolidated lacustrine sedimentation.



Figure 10. Features of disturbance layers in the drilling core.

5 Discussion

It is well known that the sporopollen is one of the palaeontology indicators which are used for climate proxies. Plants such as *Pinus*, Cupressaceae and Chenopodiaceae indicate chilliness and drought, while *Tsuga*, *Quercus*, *Ulmus* and *Corylus* plants indicate warmth and humectation. As shown in Fig. 5, arboreal sporopollen content is the most pronounced followed by shrubby and herbaceous sporopollen. The content of ferny spores and algous sporopollen is relatively low (in most case less than 10%). According to the variation of sporopollen, the whole elevation profile can be divided into nine segments (I–IX) corresponding to nine climates. In each segment, *Pinus* sporopollen dominates, followed by *Quercus* or Cupressaceae.

Segment I presents a *Pinus*-Cupressaceae-*Quercus*-Chenopodiaceae sporopollen group. According to the average content of *Pinus*, Cupressaceae, Chenopodiaceae (indicating chilliness and drought), *Quercus* and *Tsuga* (indicating warmth and humectation), the climate in this segment

would be cool and semi-humid and the vegetation represents an acerose and broadleaved-forest type.

Segment II is mainly a *Pinus*-*Quercus*-Chenopodiaceae sporopollen group. The contents of all sporopollen are relatively stable. Compared to Segment I, the content of *Pinus* and *Corylus* increased, that of *Quercus* and *Larch* obviously decreased, while that of Chenopodiaceae and *Artemisia* stay unchanged. This indicates a cold and dry climate and a vegetation of acerose-leaved-forest type.

Segment III presents a *Pinus*-*Quercus*-Cupressaceae-Chenopodiaceae sporopollen group. The content of *Pinus* obviously decreases, while that of Cupressaceae and *Quercus* increases sharply, as well as that of *Larch*. As *Quercus* indicates warmth and humectation, the climate in this segment is cool and of semi-dry and the vegetation is of the acerose and broadleaved-forest-grassland type.

Segment IV is mainly a *Pinus*-*Quercus*-Cupressaceae-*Artemisia* sporopollen group. The content of *Pinus* and Cupressaceae is basically unchanged. The content of *Larch* and Chenopodiaceae obviously decreases, while that of *Quercus*

Table 1. The palaeoclimatic periods in the study area.

Segment	Elevation of disturbance layer (a.s.l.)	Palaeoclimate and palaeoenvironment			
		Elevation (a.s.l.)	Period (a BP)	Climate	Vegetation
10	2321–2313	2323–2333	15 650–14 992	warm-humid	forest
9	2306–2300	2301–2323	16 902–15 650	warm-dry	forest–grassland
8	2291–2288	2290–2301	17 413–16 902	cool-dry	forest–grassland
7	2275–2269	2273–2290	18 531–17 413	cold-dry	forest–grassland
6	2262–2253	2229–2273	21 425–18 531	hot-dry	forest
5	2206–2200	2207–2229	22 872–21 425	warm-dry	forest
4	2193–2189	2174–2207	25 043–22 872	cold-dry	forest–grassland
3	2166–2163	2146–2174	26 916–25 043	cool-dry	forest–grassland
2	2154–2152	2115–2146	29 077–26 916	hot-humid	forest
1	2137–2134	2095–2115	30 830–29 077	warm-humid	forest

**Figure 11.** Earthquake-induced disturbance layer in the sediment exposed on an outcrop.

and *Tsuga* increases markedly. This indicates the climate in this segment is of warm and humid features with acerose and broadleaved-forest–grassland vegetation.

Segment V is mainly a *Pinus-Quercus-Cupressaceae-Chenopodiaceae* sporopollen group. The content of *Larch* and Gramineae increases slightly. The content of *Quercus* and *Tsuga* decreases. This indicates a cold and semi-dry climate with vegetation of the acerose and broadleaved-forest type.

Segment VI is a *Pinus-Quercus-Corylus-Artemisia* sporopollen group. The content of *Pinus* and Cupressaceae increases, while that of Chenopodiaceae, *Quercus* and *Tsuga* decreases markedly. This indicates a climate of warm and humid features with vegetation of the acerose-leaved-forest type.

Segment VII is a *Pinus-Quercus-Chenopodiaceae* sporopollen group. The content of *Pinus* increases, while that of *Quercus* increases, indicating a cold and semi-humid climate with vegetation of the forest–grassland type.

Segment VIII is a *Pinus-Quercus-Cupressaceae-Corylus-Gramineae* sporopollen group. The content of *Pinus* decreases, while that of *Quercus* increases, indicating a climate of cool and mid-drought features with vegetation of the acerose and broadleaved-forest–grassland type.

Segment IX is mainly a *Pinus-Quercus-Corylus-Chenopodiaceae* sporopollen group. The content of *Pinus* slightly increases, while that of *Quercus* obviously decreases, indicating a cold and dry climate with forest-type vegetation.

The climates in the above-mentioned nine segments exhibit alternate warm-humid and cold-dry climates and alternate vegetation types (forest–grassland type in segments III, IV, VII and VIII and forest type in segments I, II, V, VI and IX).

Referring to the study by Chen et al. (2000) on open freshwater lakes, we consider that the high value of $\delta^{13}\text{C}$ indicates warm climate, while the low value of $\delta^{13}\text{C}$ means cold climate. However, the high value of $\delta^{18}\text{O}$ indicates cold

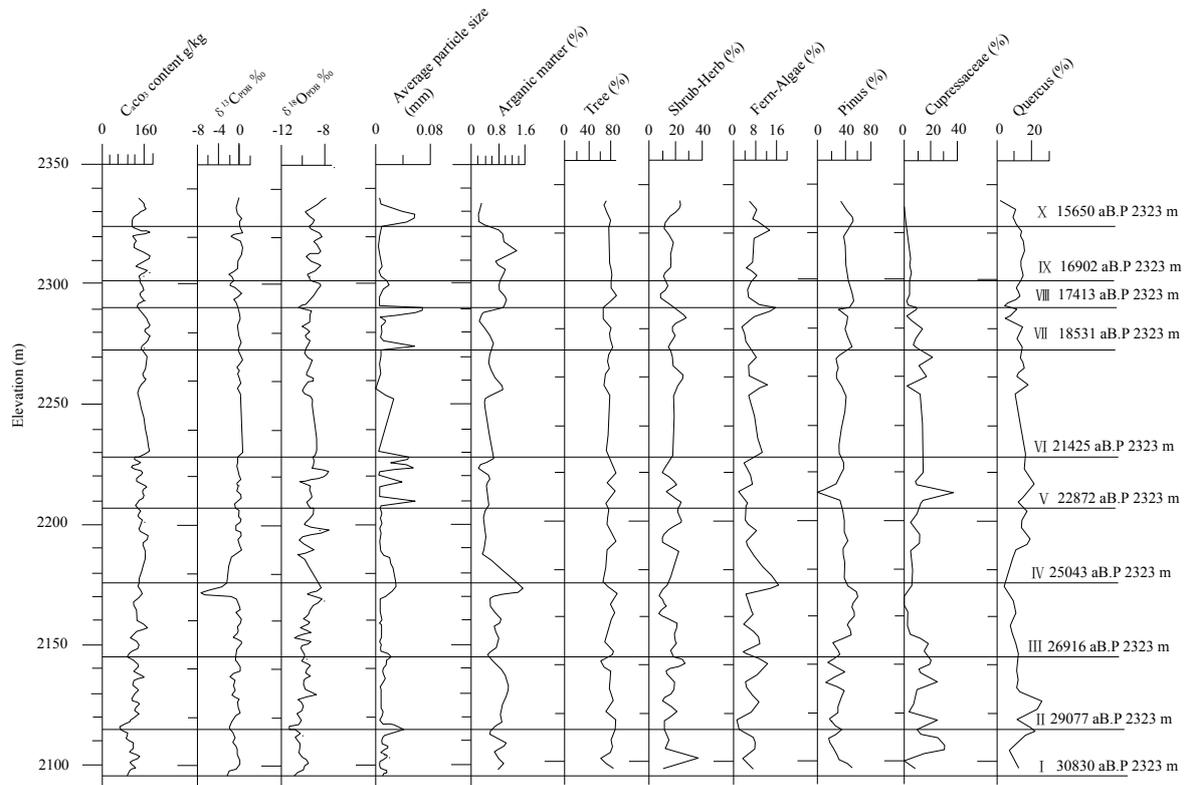


Figure 12. Delineation of palaeoclimate in the study area.

climate, while the low value means humid climate. As shown in Fig. 6, the values of $\delta^{13}\text{C}$ and $\delta^{18}\text{O}$ and their ratio fluctuate with elevation. According to the variation feature of $\delta^{13}\text{C}/\delta^{18}\text{O}$, the entire elevation profile is differentiated into 13 segments, each representing a climate type. Segments I, II, III and X indicate humid climate and others are dry. Additionally, segments I, II, IV and V reflect typical cold climates. In general, the upper part of the profile experienced somewhat warm and dry climates, while the lower part experienced relatively cold and humid climates.

The organic matter represents the enrichment of humus in soils, which is generally caused by bioorganic actions. The high percentage of the organic matter not only illustrates the accumulation of the humus, but also indicates a humid condition during the formation of soil and an active process of bioorganic action. A warm and humid climate favours luxuriant growth of vegetation, which is beneficial to the accumulation of humus. Although the content of the organic matter in the stratum would be affected by the decomposition of the organic matter itself, the content measured today still reflects the biomass values at that time. According to the variation of organic matter content in Fig. 7, the elevation profile can be differentiated into 11 segments.

Based on studies on contemporary lakes, Wang and Li (1991) indicated that a close relationship exists between the sedimentation of calcium carbonate and the climate and

environment, as the content of calcium carbonate in the sediments reflects the palaeoclimatic features in the process of forming sediments. Generally, the high CaCO_3 content represents a cold and dry climate, while the low represents a humid climate. According to this variation of CaCO_3 content in Fig. 8, the elevation profile can be differentiated into 15 segments. Segments I and II are relatively warm and humid, while segments IX, X and XIV are somewhat cold and dry.

The Diexi barrier lake is an open and drained lake and its sediments stem from materials upstream of the Minjiang River. The granularity test indicates that the sediments are mostly silty clay, clayey silt and sandy silt. The coarse grain represents plentiful rainfall, humid climate and strong hydrodynamic conditions, while the finest grains represent less rainfall, dry climate and weak hydrodynamic conditions (Chen et al., 2003). As shown in Fig. 9, the average particle sizes exhibit strong fluctuation with elevation. The variation in the lower portion of the profile is relatively small, while that in the upper portion is relatively large. According to the granularity, the entire profile can be differentiated into 11 segments. Segments I, V, VII, IX and XI indicate a relatively humid climate, while segments II, III, IV, VI, VIII and X are relatively dry.

By combining the above-mentioned individual climatic indicators and the dating results, Fig. 12 and Table 1 are obtained to summarize and delineate the palaeoclimatic history

in the Diexi area. In total, 10 climate and environment segments are identified. From about 30 830 till 26 916 a BP, the Diexi area was covered by forest vegetation and the climate changed from warm-humid to hot-humid. Since 26 916 a BP, the temperature became lower and the vegetation was of forest–grassland type. From about 22 872 a BP, the climate changed to be warm-dry and hot-dry with forest vegetation in this area. After that a cold climate came and lasted for about 1600 a (from 18 531 to 16 902 a BP) and the vegetation was forest–grassland type. From 16 902 to 14 992 a BP the temperature increased. The whole profile shows a cyclic evolution of climate from warm-humid to cold-dry.

Comparing the palaeoclimate segments in Fig. 12 and Table 1 and the disturbance zones in Fig. 10, there is a good correlation between the climatic and environmental changes and the earthquake events. It is inferred that a strong earthquake is usually accompanied by climate change. In other words, the atmosphere the climate relies on and the rock cycle the earthquake action relies on are closely associated. Based on the preliminary results from this study, we considering that the climate change and the geological and environmental evolution of the eastern edge of Tibetan Plateau may proceed cyclically at an interval of about 15 000 a, and that climate change was accompanied by seismic events. To expand on this argument, further study is required to decipher the inner correlations between the climate change and earthquake events.

6 Conclusions

The present study focuses on the Diexi barrier lake in the Minjiang River, which is located in a complex geological region. Drilling and sampling were conducted in the centre of the barrier lake. Climatic indicators were examined through an elevation profile from 2090 m to 2330 m a.s.l. to recover the palaeoclimate in this area. Based on the foregoing discussion, the main conclusions are as follows:

1. Ten climatic periods have been identified for the Diexi barrier lake area within the time span from 30 000 to 15 000 a BP, based on examination of the climatic indicators, such as spore-pollen, organic matter, carbon and oxygen isotopes, calcium carbonate and particle size.
2. Ten earthquake-induced disturbance layers in the lake sediments were identified through examination of the drilling core. This indicates that from 30 000 to 15 000 a BP, there were at least 10 strong earthquakes in the Diexi area.
3. The disturbance sections formed by earthquakes show good consistency with the climate changes, indicating that the geologic evolution and the climatic and environmental changes are associated.

Acknowledgements. This study is supported by the National Natural Science Foundation of China (no. 41072230 and 51309176) and funding from the State Key Laboratory of Geohazard Prevention and Geoenvironment Protection (SKLGP2012Z008).

Edited by: R. Lasaponara

Reviewed by: two anonymous referees

References

- An, W., Zhao, J. Q., and Yan, X. B.: Tectonic deformation of lacustrine sediments in Qiangyang on the Minjiang fault zone and ancient earthquake, *Seismol. Geol.*, 4, 980–988, 2008.
- Chen, J. A., Wan, G. J., and Tang, D. G.: Modern climate change Erhai Lake sediment grain size and isotopic records, *Nat. Sci. Prog.*, 10, 253–259, 2000.
- Chen, J. A., Wan, G. J., and Zhang, F.: Environmental record in lake sediments at different time scales – a case study in sediment grain size, *Chinese Sci. Ser. D*, 33, 563–568, 2003.
- Duan, L. P.: The Ancient Barrier Lake and Geoenvironment, Diexi, Minjiang River, Ph.D. thesis, Chengdu University of Technology, China, 2002.
- Duan, L. P., Wang, L. S., and Yang, L. Z.: The ancient climatic evolution characteristic reflected by carbon and oxygen isotopes of carbonate in the ancient barrier lacustrine deposits, Diexi, Minjiang River, *The Chinese J. Geol. Hazard Control*, 13, 91–96, 2002.
- Krivonogov, S. K., Sheinkman, V. S., and Mistryukov, A. A.: Stages in the development of the Darhad dammed lake (Northern Mongolia) during the Late Pleistocene and Holocene, *Quaternary Int.*, 136, 83–94, 2005.
- Moreiras, S. M.: Chronology of a probable geotectonic Pleistocene rock avalanche, Cordon del Plata (Central Andes), Mendoza, Argentina, *Quaternary Int.*, 148, 138–148, 2006.
- Trauth, M. H. and Strecker, M. R.: Formation of landslide-dammed lakes during a wet period between 40,000 and 25,000 yr B. P. in northwestern Argentina, *Palaeogeogr. Palaeoclimatol.*, 153, 277–287, 1999.
- Wang, L. S., Yang, L. Z., and Li, T. B.: Evolution mechanism of Jiaochang earthquake landslide on Minjiang River and its controlling, *J. Geol. Hazards Environ. Preserv.*, 11, 195–199, 2000.
- Wang, L. S., Yang, L. Z., and Wang, X. Q.: Discovery of huge ancient dammed lake on upstream of Minjiang River in Sichuan, China, *J. Chengdu University of Technology: Science and Technology Edition*, 32, 1–11, 2005.
- Wang, L. S., Wang, X. Q., and Xu, X. N.: What happened on the upstream of Minjiang River in Sichuan Province 20,000 years ago, *Earth Sci. Front.*, 14, 189–196, 2007.
- Wang, P., Zhang, B., Qiu, W. L., and Wang, J. C.: Soft-sediment deformation structures from the Diexi paleo-dammed lakes in the upper reaches of the Minjiang River, east Tibet, *J. Asian Earth Sci.*, 40, 865–872, 2011.
- Wang, S. B., Li, Y., and Xia, X. G.: Magnetostratigraphic Study of Lake Sediments in Jiaochang, Maoxian County, Sichuan, 426 pp., 2006.
- Wang, S. M. and Li, J. R.: Lake sediments – effective means to study the history of climate – an example from Qinghai Lake and Daihai Lake, *Chinese Sci. Bull.*, 36, 54–56, 1991.

- Wang, X. Q.: The Environment Geological Information in the Sediments of Diexi Ancient Dammed Lake on the upstream of Mingjiang River in Sichuan Province, China, Ph.D. thesis, Chengdu University of Technology, Chengdu, China, 2009.
- Wassmer, P., Schneider, J. L., Pollet, N., and Schmitter-Voirin, C.: Effects of the internal structure of a rock-avalanche dam on the drainage mechanism of its impoundment, Flims sturzstrom and Ilanz paleo-lake, Swiss Alps, *Geomorphology*, 61, 3–17, 2004.
- Weidinger, J. T.: Case history and hazard analysis of two lake-damming landslides in the Himalayas, *J. Asian Earth Sci.*, 16, 323–331, 1998.
- Wu, J. L., Li, S. J., and Wang, S. M.: Modern climatic signals recorded in Xincuo Lake sediments in Zoige Basin, eastern Tibetan plateau, China, *J. Lake Sci.*, 12, 291–296, 2000.
- Yang, W. G.: Research of sedimentary record in terraces and climate vary in the upper reaches of Mingjiang River, china, Ph.D. thesis, Chengdu University of Technology, Chengdu, China, 2005.
- Zhang, Y., Zhu, L., and Yang, W., Luo, H., He, D., and Liu, J.: High resolution rapid climate change records of lacustrine deposits of Diexi Basin in the eastern margin of Qinghai-Tibet Plateau, 40–30 ka BP, *Earth Sci. Front.*, 5, 91–98, 2009.
- Zhao, X. T., Qu, Y. X., and Zhang, Y. S.: Discovery of Shigu Paleolake in the Lijiang area, northwestern Yunnan, China and its significance for the development of the modern Jinsha River valley, *Geol. Bull. China*, 8, 960–969, 2007.
- Zhu, D. G., Meng, X. G., and Zhao, X. T.: Lake-level change of Namco Tibet since the Late Pleistocene and environment information of clay minerals in lacustrine deposits, *J. Geomechan.*, 10, 300–309, 2004.